Soft Matter

Cite this: *Soft Matter*, 2011, **7**, 6061

www.rsc.org/softmatter

PAPER

The effect of the Hofmeister series on the deswelling isotherms of poly(*N*-isopropylacrylamide) and poly(*N*,*N*-diethylacrylamide)

Leena Patra,† Ajay Vidyasagar† and Ryan Toomey*

Received 10th February 2011, Accepted 21st April 2011
DOI: 10.1039/c1sm05222e

The influence of Na_2SO_4, NaCl, NaBr, and NaI was studied on the deswelling isotherms of thin films of photo-crosslinked poly(*N*-isopropylacrylamide) and poly(*N*,*N*-diethylacrylamide) to help elucidate the mechanisms by which ions of the Hofmeister series affect the solubility of neutral, amide-based polymers. The films were characterized with both ellipsometry and FTIR to determine both water content and the frequency of the C=O, N–H, and CH_3 vibrations associated with the polymers. When compared at the same water content, the frequency of the N–H bend in poly(NIPAAm) red-shifts in the order $I^- > Cl^- > Br^- > SO_4^{2-}$. The red-shift is consistent with disrupted hydrogen bonding of the N–H moiety due to an ion–dipole attraction. The C=O stretch on the other hand is insensitive to the ion, suggesting that the ion pairs primarily with the partially positive end of the HN–C=O dipole. For poly (DEAAm), which lacks an N–H moiety, the C=O stretch is now sensitive to the ion, with the trend following the order of the ion in the Hofmeister series. Both of these findings signify that $I^- > Cl^- > Br^- > SO_4^{2-}$ with respect to the strength of the ion–dipole interaction. Moreover, the ion–dipole interaction is stronger in poly(NIPAAm) than poly(DEAAm), suggesting that the specificity of the Hofmeister ions arises from the effect of vicinal groups on the amide dipole.

I. Introduction

Lower critical solution temperature (LCST) polymers can serve as model systems for probing the effect of ions on the stability of biological macromolecules.[1–4] It is well established that the dissolution temperature of LCST polymers, including poly(*N*-isopropylacrylamide), or poly(NIPAAm), is strongly affected by the addition of salt, in a manner similar to how protein stability is affected by salt.[5–13] The effect of ions, however, is not purely concentration dependent. The dissolution temperature depends on the "structure forming" or "structure breaking ability" of the ion and follows the Hofmeister series.[14–17]

LCST polymers contain a hydrogen-bonding group, such as an amide, and a hydrophobic group. At low temperatures, solubility of the macromolecule is engendered through favorable mixing of the hydrogen-bonding groups and water. As temperature is increased, a point is reached where mixing can no longer stabilize hydrophobic interactions and the polymer phase-separates from solution.

Despite a considerable body of research, however, questions still remain concerning the exact mechanism of the interaction of salts with macromolecules that contain both amides and hydrophobic groups. It is generally thought that the effect of the Hofmeister salts result from ion-specific interactions with both amide and nonpolar moieties,[14] where the amide interaction is perhaps a nonspecific ion–dipole interaction that is modulated by vicinal methyl groups.[18] Cremer and co-workers proposed that strong "salting out" salts act by polarizing the water molecules adjacent to the amide groups and by increasing the surface tension around the hydrophobic groups, while "salting in" salts bind directly to the amide groups.[7] They also suggested a two-step demixing process for strong salting out anions like SO_4^{2-}, wherein amide groups are first dehydrated followed by the dehydration of the isopropyl groups.[7]

Near the water/air interface, all ions of the Hofmeister series increase surface tension due to exclusion of the ions near the surface.[19,20] Similar effects have been observed with the salting out of benzene from aqueous solution, where ions decrease the solubility of benzene in water.[21] It may therefore be expected that all macromolecules have decreased solubility in salt solutions. Indeed, early members of the Hofmeister series, or kosmotropes, do monotonically decrease solubility. Later members of the Hofmeister series, or chaotropes, however, can form ion–dipole pairs with hydrogen bonding moieties and increase solubility.[22–24]

In this paper, we explore the influence of Na_2SO_4, NaCl, NaBr, and NaI on the swelling of thin layers of surface-attached networks of poly(NIPAAm) and poly(*N*,*N*-diethylacrylamide), or poly(DEAAm), both of which are amide-based polymers. Poly (NIPAAm) contains a secondary amide that donates and accepts a hydrogen bond; whereas, poly(DEAAm) contains a tertiary

Department of Chemical and Biomedical Engineering, University of South Florida, Tampa, FL, 33620, USA. E-mail: toomey@usf.edu
† Both authors contributed equally.

amide that only accepts a hydrogen bond. The Hofmeister series suggests that $SO_4^{2-} > Cl^- > Br^- > I^-$ in terms of the anion's ability to salt-out neutral, LCST polymers. Within this ordering, SO_4^{2-} is kosmotropic, I^- is chaotropic, and Cl^- and Br^- are intermediate. We use both ATR-FTIR and ellipsometry to characterize the surface-attached networks. While FTIR has been extensively used to measure the frequency shifts of the vibrations associated with the amide and aliphatic groups in LCST polymers and gels upon demixing,[25–29] interpretation of spectra is difficult without precise knowledge of the water content. To that end, we use ellipsometry to derive the average water distribution in the polymer coatings. FTIR spectra are then compared at the same water content in order to unambiguously determine the effect of ions on the vibrations of the amide and aliphatic groups.

II. Experimental section

Materials

N-Isopropylacrylamide (NIPAAm), *N*,*N*-diethylacrylamide (DEAAm), 4-hydroxybenzophenone, methacryloyl chloride, triethylamine, acetone, D_2O (99.9 atom%), Na_2SO_4, NaCl, NaBr, NaI, azobisisobutyronitrile (AIBN), hexanes, diethyl ether and 3-aminopropyl triethoxysilane were purchased from Sigma. Acetone was distilled from calcium hydride before use and NIPAAm was recrystallized from hexanes. All other chemicals were used as received.

Monomer synthesis

Methacryloyloxybenzophenone (MaBP) was synthesized from 4-hydroxybenzophenone and methacryloyl chloride in dry acetone at 0 °C as described previously.[30] The monomer yield was around 90% MaBP and characterized with an INOVA 400 NMR spectrometer. The spectrum had typical aromatic peaks (multiplet) at 7.2–8.0(m) ppm and a singlet at 2.1(s) ppm representing the methyl group characteristic of MaBP.

Copolymer synthesis

Poly(NIPAAm-*co*-MaBP) or poly(DEAAm-*co*-MaBP) was copolymerized with 3 mol% MaBP using 0.1% AIBN as the initiator. Several samples were prepared. All reactions were carried out for 18 hours at 65 °C in dioxane under nitrogen. The samples were degassed with nitrogen by freeze and thaw cycles prior to the reaction. After completion, the polymer was precipitated in diethyl ether. To verify incorporation of MaBP, ^{1}H NMR in $CDCl_3$ was conducted. The percentage of MaBP was calculated from the integration of the CH peaks of the aromatic group (7.2–8.0(m) ppm) and the integration CH peaks of the isopropyl group of NIPAAm or the diethyl group of DEAAm in the NMR spectrum with an error estimate of 5%. All samples showed complete incorporation of the MaBP. GPC on all samples were performed on a Viscotek™ using RI, VIS, RALS, and LALS. Molecular weights were determined by the triple detection method. The number-average molecular weight of poly(NIPAAm-*co*-MaBP) is 42 830 g mol^{-1} with a polydispersity of 4.7. The number-average molecular weight of poly(DEAAm-*co*-MaBP) is 13 342 g mol^{-1} with a polydispersity of 2.39.

Preparation of surface-tethered network for ellipsometry

LaSFN9 prisms were cleaned with ozone to remove any organic impurities followed by deposition in a 1% solution of 3-aminopropyl triethoxysilane in acetone. The substrates were heated to 100 °C to drive condensation of the silane groups to the substrate surface. A solution of the appropriate polymer in cyclohexanone was spin cast on the freshly prepared substrate. Crosslinking was accomplished by exposing the film to UV light (365 nm) for 30 minutes. Ultraviolet radiation (λ = 365 nm) triggers the n,π^* transition in the benzophenone moieties leading to a biradicaloid triplet state that abstracts a hydrogen from a neighboring aliphatic C–H group, forming a stable C–C bond. The coatings were subsequently solvated in water and/or salt solutions for 30 minutes, enough time to attain homogeneity of the coating throughout its thickness.

Ellipsometry

The dry and swollen profiles of the surface-attached films were measured with a home-built variable-angle nulling ellipsometer in an ATR configuration. The light-source was a He–Ne laser with a wavelength of λ = 633 nm. The experimental setup has been described in detail elsewhere.[31] The refractive index of the LaSFN9 prism is $n = 1.845$, and in contact with water, the critical angle of total reflection is 46.7°. The thickness of all films was in the optical range, giving rise to sufficient features in the recorded spectra to infer the refractive index profile. To analyze the data, model refractive index profiles were generated, and the ellipsometric parameters were numerically calculated using the matrix optical formulation.[32] The parameters of the model were adjusted to minimize the differences between the simulation and experimental data.

ATR-FTIR

ATR-FTIR measurements of poly(NIPAAm-*co*-MaBP) or poly(DEAAm-*co*-MaBP) were performed using a Nicolet 6700 FTIR spectrometer equipped with a temperature controlled multi-bounce ATR ZnSe plate. The polymers dissolved in acetone were cast onto the ZnSe plate and heated to 60 °C for 2 hours to remove residual acetone. An FTIR spectrum was then performed to determine that there was no residual acetone left in the polymer cast on the ZnSe plate. All FTIR measurements were performed at 24 °C in absorbance mode with 100 scans and a resolution of 4 cm^{-1}. The spectral ranges for all scans were in the region between 4000 and 650 cm^{-1}. The crystal background was subtracted from the samples for each run.

III. Results

Fig. 1 shows the thermally induced deswelling transition (or deswelling isobars) in both poly(NIPAAm) and poly(DEAAm) networks with 3 mole% MaBP cross-linker. Both have a demixing temperature near 30 °C. Below the deswelling temperature, poly(NIPAAm) has a higher equilibrium water content than poly(DEAAm), which is likely the result that poly(NIPAAm) can hydrogen bond to water at both the C=O and N–H positions whereas poly(DEAAm) can hydrogen bond at the C=O position. Interestingly, the two ethyl groups of poly(DEAAm) do not

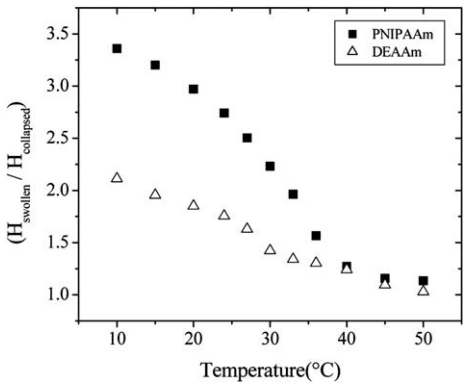

Fig. 1 Deswelling isobars of poly(NIPAAm) and poly(DEAAm) showing a demixing temperature near 30 °C.

alter the transition temperature with respect to poly(NIPAAm); however, the deswelling isobar is more gradual than in poly (NIPAAm).

Fig. 2 shows the deswelling isotherms, or the variation in the dimensionless thickness of both poly(NIPAAm) and poly (DEAAm), over a range of salt concentrations (0–2.0 M) for Na_2SO_4 (Fig. 2a), NaCl (Fig. 2b), NaBr (Fig. 2c), and NaI (Fig. 2d), all carried out at 5 °C. The dimensionless thickness is defined as $(H - H_{collapsed})/(H_{swollen} - H_{collapsed})$, where H is the thickness at the respective salt concentration, $H_{swollen}$ is the thickness in water at 5 °C and $H_{collapsed}$ is the thickness at 42 °C. Comparing poly(DEAAm) and poly(NIPAAm), despite the difference in the collapse profiles with respect to temperature, they display similar collapse profiles with each salt. If a salt concentration $C_{1/2}$ is defined for when the polymer layer reaches a dimensionless thickness value of $^1/_2$, the values of $C_{1/2}$ for Na_2SO_4, NaCl and NaBr, are 0.25 M, 1.3 M, and 2.5 M, respectively, for both poly(DEAAm) and poly(NIPAAm). At 5 °C, a $C_{1/2}$ for NaI, could not be found up to 5.0 M. NaI also leads to slight additional swelling of both layers (by ~5 to 10%) at low salt concentrations.

The air/water surface tension increments of the individual salts in dynes/(cm × molality) are $Na_2SO_4 = 2.77$, NaCl = 1.73, NaBr = 1.47, and NaI = 1.14.[19] Hence, based on the values of $C_{1/2}$ previously mentioned, it becomes readily apparent that the air/water surface tension increments of the individual ions cannot be used to predict deswelling behavior. An argument based solely on air–surface tension increment would suggest that $C_{1/2}$ for NaCl would be 2.77/1.73 or 1.6 times the value $C_{1/2}$ for Na_2SO_4. Likewise, NaBr and NaI would be 1.9 and 2.4 times the value of Na_2SO_4, respectively. The fact that each of these ratios underpredicts the experimentally observed values suggests that ions may be directly interacting with the polymer, perhaps through a dipole–ion interaction that stabilizes the swollen network.

By changing the temperature of the experiment, the subtle effects of the ions can be distinctly observed. Fig. 3 and 4 show similar experiments conducted at 15 and 24 °C. At both temperatures, the deswelling isotherms for poly(NIPAAm) and poly (DEAAm) overlap in Na_2SO_4 and NaCl. However, the ratio of $C_{1/2}$ at 5 °C to $C_{1/2}$ at 24 °C is different for the two salts. The value of $C_{1/2}$ for Na_2SO_4 at 5 °C (Fig. 2a) is 2.2 times the value at 24 °C (Fig. 4a); whereas, the value of $C_{1/2}$ for NaCl at 5 °C (Fig. 2b) is 3

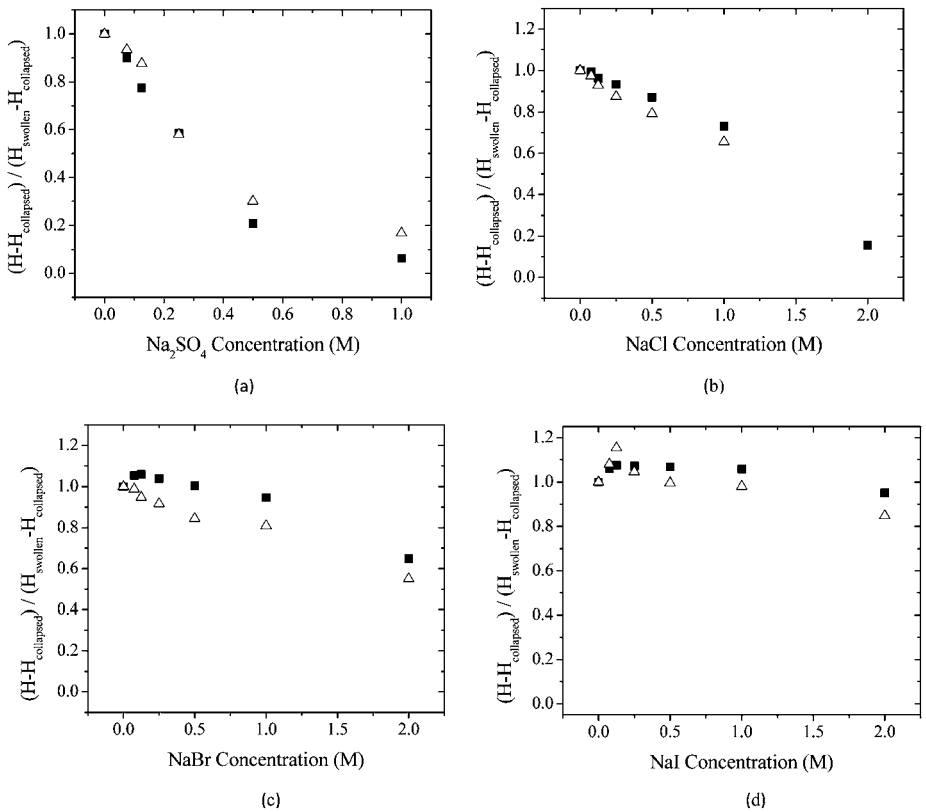

Fig. 2 Variation in thickness of poly(NIPAAm) (■) and poly(DEAAm) (△) at 5 °C in between 0 and 2.0 M salt concentration for (a) Na_2SO_4; (b) NaCl; (c) NaBr; and (d) NaI.

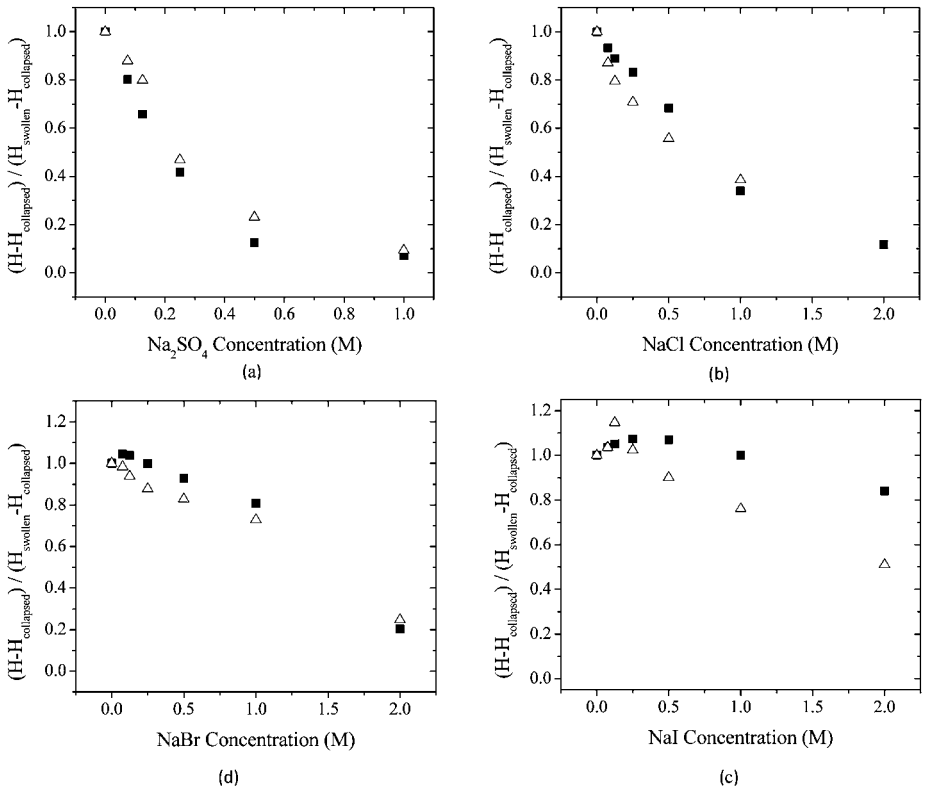

Fig. 3 Variation in thickness of poly(NIPAAm) (■) and poly(DEAAm) (△) at 15 °C in between 0 and 2.0 M salt concentration for (a) Na_2SO_4; (b) NaCl; (c) NaBr; and (d) NaI.

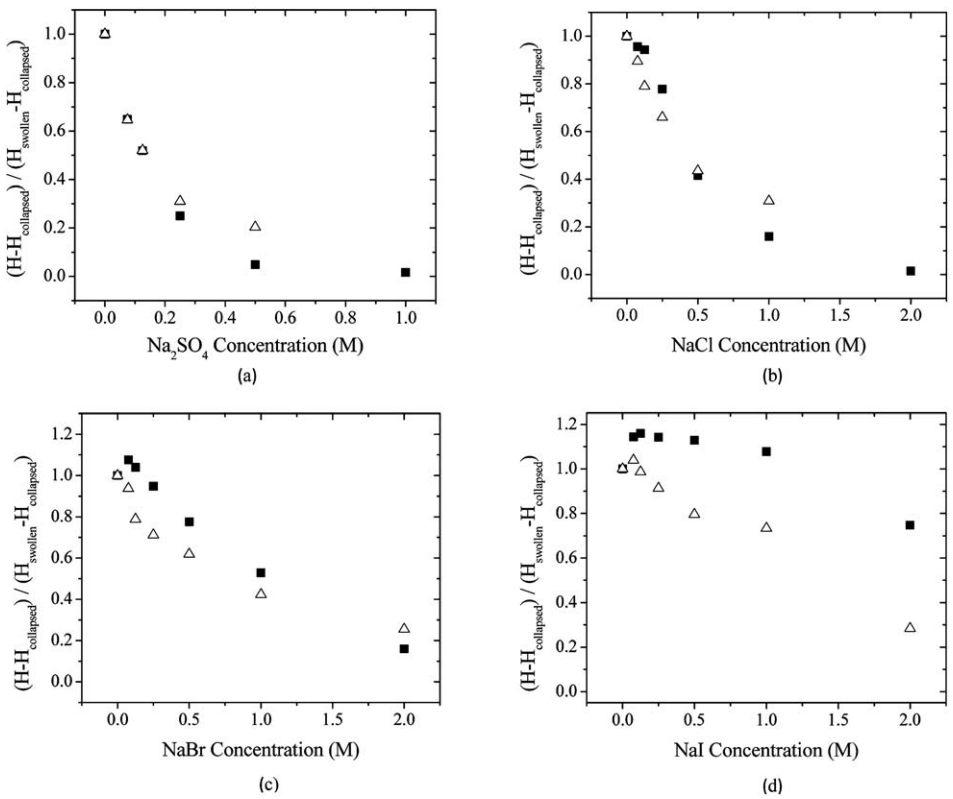

Fig. 4 Variation in thickness of poly(NIPAAm) (■) and poly(DEAAm) (△) at 24 °C in between 0 and 2.0 M salt concentration for (a) Na_2SO_4; (b) NaCl; (c) NaBr; and (d) NaI.

times the value at 24 °C (Fig. 4b). This may be due to an increasingly stronger interaction of Cl^- with the amide than SO_4^{2-} as the temperature is increased.

For NaBr, there is a small difference in deswelling isotherms of poly(DEAAm) and poly(NIPAAm) at 15 °C, where NaBr is perhaps slightly more effective at salting-out poly(DEAAm). This difference becomes significant, however, at 24 °C, where $C_{1/2}$ for poly(NIPAAm) is 1.0 M and for poly(DEAAm) it is 0.7 M. Moreover, a slight salting-in effect is measured for poly (NIPAAm), which increases with temperature. At 24 °C, the maximum degree of salting-in is 8%.

With respect to NaI, there is considerable deviation in the deswelling isotherms for poly(NIPAAm) and poly(DEAAm), with the deviation becoming more prominent as the temperature is increased. At both 15 and 24 °C, NaI is more effective at deswelling poly(DEAAm) than poly(NIPAAm). Moreover, NaI salts-in poly(NIPAAm) at low salt concentrations, with the degree of salting-in increasing with temperature. In contrast, the opposite trend is seen with poly(DEAAm), where the degree of salting-in decreases with temperature. That said, the maximum degree of salting-in is 5% for poly(DEAAm) at 5 °C and 18% for poly(NIPAAm) at 24 °C.

It was noted that that the bulk surface tension increments of the individual salts are insufficient to quantitatively interpret the deswelling isotherms. It is tempting to explain the deviation with respect to a difference in the partitioning of ions between the macromolecule surface and bulk water and the partitioning ions between an air interface and bulk water interface. At the air/water interface, ions that possess a large charge/volume ratio are generally excluded from the interface, as they are less likely to give up their hydration waters.[19,33] Ions with a smaller charge/volume ratio can more easily forfeit their hydration waters and therefore are able to access the interfacial zone. A question is how the presence of dipoles influences ion partitioning. Towards this end, we use ATR-FTIR to study the amide group and aliphatic CH_3 vibrations of poly(NIPAAm) and poly(DEAAm) upon exposure to salt.

Fig. 5 shows the FTIR and the associated 2nd derivative spectrum of the amide I and amide II regions of poly(NIPAAm) in pure water at both 24 and 50 °C. The amide I vibration, absorbing near 1650 cm^{-1}, arises mainly from the C═O stretching vibration with minor contributions from the out-of-phase CN stretching vibration, the C–C–N deformation and the N–H in-plane bend. The amide II mode is the out-of-phase combination of the N–H in-plane bend and the C–N stretching vibration with smaller contributions from the C═O in-plane bend and the C–C and N–C stretching vibrations. As a general rule, hydrogen bonding lowers the frequency of amide I since it lowers the restoring force of the C═O stretching vibration, but increases the frequency of amide II since it produces an additional restoring force.[34]

At 24 °C, the amide I peak consists of one band that is centered at 1625 cm^{-1} and the amide II consists of one band at 1558 cm^{-1}. As temperature is increased to 50 °C, both bands shift to lower frequencies. A distinct sub-band arises, however, at 1651 cm^{-1} in the amide I region. It is believed that this band arises due to the hindered ability of carbonyl moiety to hydrogen bond water, which increases the electron density leading to a higher stiffness. Hence, upon increasing temperature, the overall amide I peak first decreases in frequency followed by an increase in frequency due to the rise in the sub-band. The amide II, in contrast, does not develop and secondary bands and shifts monotonically towards lower frequencies. It is thought that as the layer collapses, the N–H group, like the C═O group, can no longer adopt a conformation for optimal hydrogen bonding, and hence the frequency of N–H bending vibrations is lowered due to a lower restoring force. We have previously shown that in a collapsed layer, 2–3 water molecules per segment remain and that the amide hydrogens are readily exchanged with deuterium.[35] This suggests the relative absence of the intermolecular hydrogen-bonding between C═O and N–H moieties.

As the frequency of the vibrations is clearly influenced by the amount of water in the network, rather than comparing the frequencies as a function of salt concentration, we compare the vibrational frequency at the same degree of swelling for each salt, as determined from the ellipsometry measurements.

Fig. 6 shows the frequency of the amide I of poly(NIPAAm) *versus* degree of swelling in Na_2SO_4, NaCl, NaBr, and NaI at 24 °C. In all cases the amide I shows an initial decrease in the vibration frequency as salt is added followed by an increase in the frequency as the layer collapses, which is caused by the rise of the sub-band around 1651 cm^{-1}. The frequency trends for all salts overlap (to within +/− 0.5 cm^{-1}); hence, the frequencies of the vibrations appear independent of ion and depend only on the degree of swelling. In contrast, Fig. 7 shows the amide II, where now the frequencies no longer overlap. Most notably at a degree of swelling ($H/H_{collapsed}$) of 2.4, a frequency of 5 cm^{-1} separates

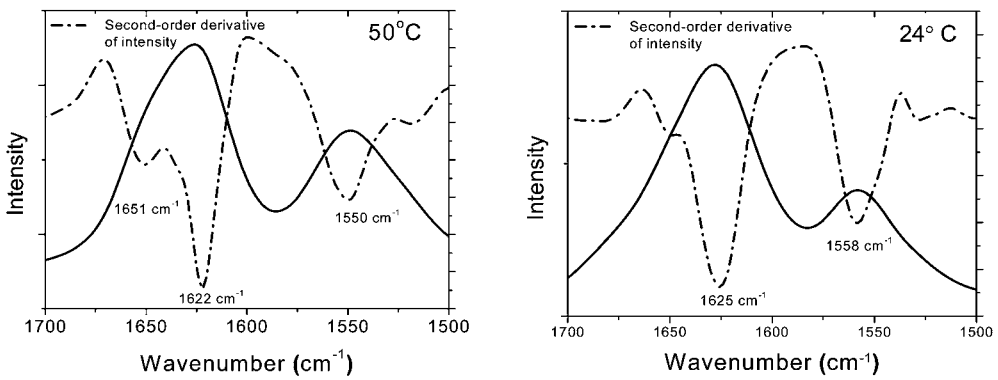

Fig. 5 FTIR spectra of the amide I and amide II vibrations of poly(NIPAAm) in water at 50 °C and 24 °C.

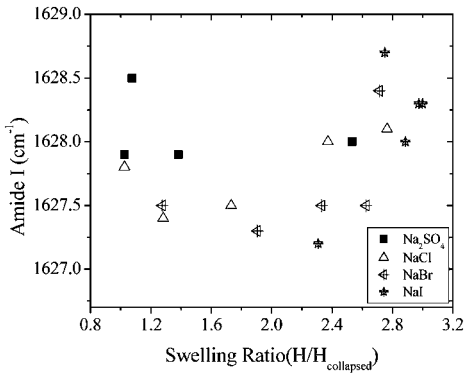

Fig. 6 Frequency shift of Amide I band as a function of degree of swelling of poly(NIPAAm) at 24 °C from 0–2.0 M salt concentrations.

NaI (1551 cm^{-1}) and Na_2SO_4 (1555 cm^{-1}). The corresponding degree of swelling in pure water occurs at 30 °C, where the position of the amide II is centered at approximately 1555 cm^{-1}, the same position of Na_2SO_4. While the proximity of the two vibrations suggests negligible interaction of Na_2SO_4 with the amide, a direct comparison is probably inappropriate due to the different temperatures of the experiment (24 °C *vs.* 30 °C). That said, for all values of $H/H_{collapsed}$ above unity, the amide II vibration of poly(NIPAAm) is lowest in NaI, followed by NaBr, NaCl and then Na_2SO_4. Interestingly, the trend follows the order of the Hofmeister series.

We speculate that the ions are electrostatically attracted to the O=C–N dipole and destabilize or sterically inhibit hydrogen bonding at the N–H moiety, decreasing the amide II frequency. NaI, which exhibits the largest effect, thus displays the largest ion–dipole attraction, which correlates with the salting-in effect measured with ellipsometry. Moreover, the trend in the vibration frequencies could explain the increase in the bulk air/water surface tension at $C_{1/2}$ for each of the salts; in other words, the stronger the ion–dipole attraction, the greater the required surface tension to collapse the layer. As the frequency of amide I is unaffected by the type of ion, it is presumed that binding or attraction is primarily between the anion and the partially positive end of the O=C–N and does not affect hydrogen bonding to the partially negative O=C end of the dipole.

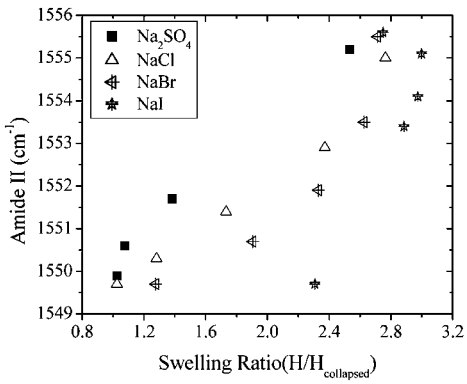

Fig. 7 Frequency shift of Amide II band as a function of degree of swelling of poly(NIPAAm) at 24 °C from 0–2.0 M salt concentrations.

In poly(DEAAm) (which lacks a N–H moiety), the frequency of the amide I vibration now depends strongly on the ion (Fig. 8). The vibration associated with Na_2SO_4 displays the same U-shape trend as seen in poly(NIPAAm), which is quite close to the frequency trend in pure water upon collapse. In NaCl, the depth of the minimum in the U-shape becomes shallower. In NaBr and NaI, the minimum disappears and now the frequency increases monotonically with temperature. We now speculate that in the case of poly(DEAAm), ions interact primarily with the partially positive end of C=O dipole. The interaction weakens the ability of the C=O to hydrogen bond with water and shifts the frequency of the vibration to higher frequencies. As in the case of the amide II vibration in poly(NIPAAm), the strength of the interaction follows the Hofmeister series. The proposed dipole–ion interactions for both poly(NIPAAm) and poly(DEAAm) are shown in Fig. 9.

Finally, it is of note to examine the CH_3 asymmetric stretching vibration in both poly(DEAAm) and poly(NIPAAm). This vibration was chosen as it is the most prominent of all the aliphatic vibrations, it shows a relatively large shift upon collapse (8 cm^{-1}), and it provides a direct comparison of the 2 terminal carbons of the isopropyl group with the 2 terminal carbons of the ethyl groups. The CH_3 asymmetric vibrations are shown in Fig. 10 as a function of salt for both poly(NIPAAm) and poly(DEAAm). The CH_3 asymmetric stretching vibration collapses to the same curve for all the salts, with the exception of poly(DEAAm) in NaI. The relative independence of the CH_3 asymmetric stretching vibration on the salt ion suggests negligible accumulation of ions on the hydrophobic surface, as expected from bulk air/water surface tension measurements. Mysteriously, however, NaI causes an increase of 3 cm^{-1} in the CH_3 vibration in poly(DEAAm), which is not observed in poly(NIPAAm). The increase may be

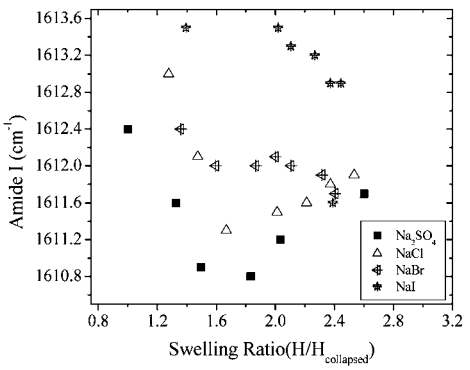

Fig. 8 Frequency shift of Amide I band as a function of degree of swelling of poly(DEAAm) at 24 °C from 0–2.0 M salt concentrations.

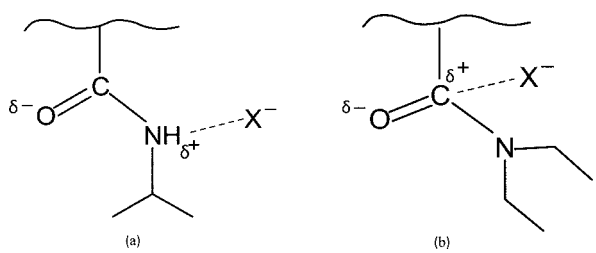

Fig. 9 Proposed sites of the amide–ion interaction in both (a) poly(*N*-isopropylacrylamide) and (b) poly(*N*,*N*-diethylacrylamide).

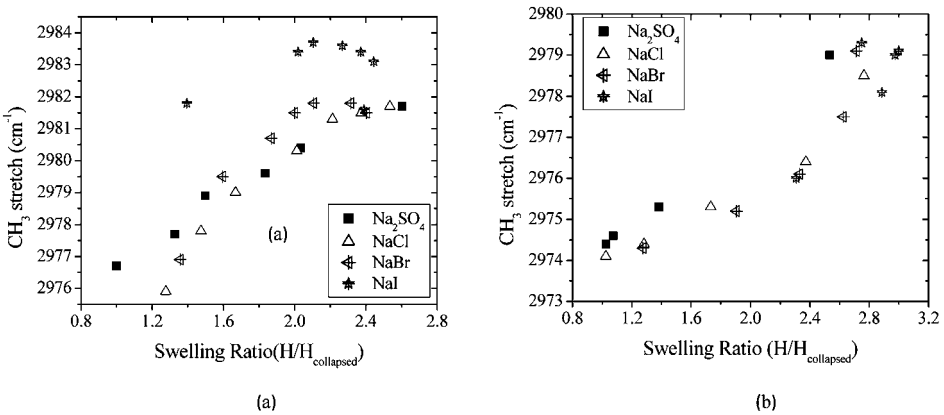

Fig. 10 CH_3 stretch vibrations as a function of degree of swelling at 24 °C from 0–2.0 M salt concentrations for (a) poly(DEAAm) and (b) poly (NIPAAm).

a consequence of the close proximity between an iodide and the CH_3 group resulting from attraction of the ion to the amide dipole. In contrast, the amide in poly(NIPAAm) is less sterically hindered and may better accommodate an iodide without perturbation of the CH_3 vibration.

IV. Conclusions

The mechanisms by which ions affect the solubility of neutral macromolecules remain unresolved. Herein, we explored the deswelling isotherms of both poly(NIPAAm) and poly(DEAAm) induced through the addition of Na_2SO_4, NaCl, NaBr, and NaI. In the presence of early members of the Hofmeister series, the demixing isotherms of both poly(NIPAAm) and poly(DEAAm) are identical. Later members of the Hofmeister series, in contrast, impart distinct deswelling isotherms for poly(NIPAAm) and poly (DEAAm), due to differences in accumulation of ions at the amide dipole. The strength of the ion–dipole interaction appears to be dictated by surrounding hydrophobicity or steric hindrance of the amide, as later members of the Hofmeister series collapse poly (DEAAm) more quickly than poly(NIPAAm). Finally, the relative absence of a dependence on the CH_3 shift and ion suggests that ions do not adsorb to the hydrophobic moieties. The one exception is NaI and poly(DEAAm), which may not arise from adsorption but close proximity of the ion to the diethyl groups due to interaction with the amide dipole.

Acknowledgements

This work was supported in part by Camille and Henry Dreyfus Foundation and NSF DMR-064557.

References

1 P. H. Von Hippel and T. Schleich, *Acc. Chem. Res.*, 1969, **2**, 257–265.
2 Y. J. Zhang and P. S. Cremer, *Curr. Opin. Chem. Biol.*, 2006, **10**, 658–663.
3 J. E. Kinsella and D. Srinivasan, *J. Biol. Chem.*, 1981, **256**, 3394–3398.
4 M. J. Hey, J. M. Clough and D. J. Taylor, *Nature*, 1976, **262**, 807–809.
5 R. Freitag and F. Garret-Flaudy, *Langmuir*, 2002, **18**, 3434–3440.
6 Y. Zhang, S. Furyk, L. B. Sagle, Y. Cho, D. E. Bergbreiter and P. S. Cremer, *J. Phys. Chem. C*, 2007, **111**, 8916–8924.
7 Y. J. Zhang, S. Furyk, D. E. Bergbreiter and P. S. Cremer, *J. Am. Chem. Soc.*, 2005, **127**, 14505–14510.
8 T. G. Park and A. S. Hoffman, *Macromolecules*, 1993, **26**, 5045–5048.
9 H. Inomata, S. Goto, K. Otake and S. Saito, *Langmuir*, 1992, **8**, 687–690.
10 E. Sedlák, L. Stagg and P. Wittung-Stafshede, *Arch. Biochem. Biophys.*, 2008, **479**, 69–73.
11 H. G. Schild and D. A. Tirrell, *J. Phys. Chem.*, 1990, **94**, 4352–4356.
12 W. Kunz, P. Lo Nostro and B. W. Ninham, *Curr. Opin. Colloid Interface Sci.*, 2004, **9**, 1–18.
13 L. Vrbka, P. Jungwirth, P. Bauduin, D. Touraud and W. Kunz, *J. Phys. Chem. B*, 2006, **110**, 7036–7043.
14 R. L. Baldwin, *Biophys. J.*, 1996, **71**, 2056–2063.
15 L. M. Pegram and M. T. Record, *J. Phys. Chem. B*, 2008, **112**, 9428–9436.
16 F. Hofmeister, *Arch. Exp. Pathol. Pharmakol.*, 1888, **24**, 247–260.
17 A. Voet, *Chem. Rev.*, 1936, **20**, 169–179.
18 A. Hamabata and P. H. Vonhippel, *Biochemistry*, 1973, **12**, 1264–1271.
19 L. M. Pegram and M. T. Record, *J. Phys. Chem. B*, 2007, **111**, 5411–5417.
20 P. B. Petersen and R. J. Saykally, *Annu. Rev. Phys. Chem.*, 2006, **57**, 333–364.
21 W. F. Mcdevit and F. A. Long, *J. Am. Chem. Soc.*, 1952, **74**, 1773–1777.
22 P. K. Nandi and D. R. Robinson, *J. Am. Chem. Soc.*, 1972, **94**, 1299.
23 O. S. Lawal, *Food Chem.*, 2006, **95**, 101–107.
24 T. H. Plumridge and R. D. Waigh, *J. Pharm. Pharmacol.*, 2002, **54**, 1155–1179.
25 Y. Maeda, T. Nakamura and I. Ikeda, *Macromolecules*, 2001, **34**, 1391.
26 A. Percot, X. X. Zhu and M. Lafleur, *J. Polym. Sci., Part B: Polym. Phys.*, 2000, **38**, 907.
27 E. Kesselman, O. Ramon, R. Berkovici and Y. Paz, *Polym. Adv. Technol.*, 2002, **13**, 982–991.
28 Y. Maeda, T. Nakamura and I. Ikeda, *Macromolecules*, 2002, **35**, 10172–10177.
29 Y. Paz, E. Kesselman, L. Fahoum, I. Portnaya and O. Ramon, *J. Polym. Sci., Part B: Polym. Phys.*, 2004, **42**, 33–46.
30 A. Vidyasagar, J. Majewski and R. Toomey, *Macromolecules*, 2008, **41**, 919–924.
31 J. Habicht, M. Schmidt, J. Ruhe and D. Johannsmann, *Langmuir*, 1999, **15**, 2460–2465.
32 M. W. Born and E. Wolf, *Principles of Optics*, University Press, Amsterdam, 1997.
33 K. D. Collins, *Biophys. J.*, 1997, **72**, 65–76.
34 N. B. Colthup, L. H. Daly and S. E. Wiberley, *Introduction to Infrared and Raman Spectroscopy*, Academic Press, New York, 1990.
35 A. Vidyasagar, H. L. Smith, J. Majewski and R. G. Toomey, *Soft Matter*, 2009, **5**, 4733–4738.